A measurement of the structure of the superionic conductor copper(I) bromide in its liquid phase by neutron diffraction

1992 J. Phys.: Condens. Matter 4 6029

(http://iopscience.iop.org/0953-8984/4/28/004)

J. Phys.: Condens. Matter 4 (1992) 6029–6038. Printed in the UK

A measurement of the structure of the superionic conductor copper(I) bromide in its liquid phase by neutron diffraction

D A Allen and R A Howe†

Department of Physics and Astronomy, University of Leicester, University Road, Leicester LE1 7RH, UK

Received 20 January 1992

Abstract. The scattering of thermal neutrons from samples of molten CuBr has been measured on the D4B liquids diffractometer at the Institut Laué–Langevin, Grenoble. The three partial structure factors and pair distribution functions for this liquid have been determined by isotopic substitution of copper. The investigation reveals a featureless cation–cation partial structure factor and distribution function, and a considerable degree of first-shell penetration by the copper ions. Similarities of the cation–cation structure to that previously found for CuCl, and evidence of an even greater cation mobility, are consistent with a reduced charge transfer model for these liquids which melt from a superionic phase.

1. Introduction

The first neutron diffraction experiment using isotopic substitution on a molten salt was that of Page and Mika (1971) on CuCl. The most significant feature of their results was the broad, featureless and heavily damped partial structure factor of Cu–Cu which, unlike the cation–cation structure factors subsequently found for the alkali halides (for example, NaCl by Edwards *et al* 1975), contrasts strongly with the highly structured anion–anion structure factors. Subsequent measurements by Eisenberg *et al* (1982) have confirmed that this behaviour is genuine and not simply an artefact of the relatively low statistics and limited range of momentum transfer of the early study. Attempts to explain this behaviour in terms of the formation of chemical species or compound formation (Powles 1975) have proved unsatisfactory. Indeed, the evidence from electrical conductivity and observed nuclear relaxation times (Boyce and Mikkelsen 1977) are consistent with an ionic description. Other attempts to explain the observed behaviour using models that include reduced ionic charges and variable ionic sizes have been tried (Ginoza *et al* 1987, Stafford *et al* 1990). However, these did not prove satisfactory when compared with the experimental results.

Ginoza *et al* pointed out that if progress in modelling its structure is to be made, proper attention would have to be given to the fact that CuCl melts from a superionic phase. They suggested that a similarly featureless cation–cation partial structure factor should be present for the melts of other salts that exhibit superionic behaviour, such as CuBr, CuI and AgI. The results of a diffraction study by Wood *et al* (1988) of NiI_2 which, in a separate inelastic scattering experiment (Wood 1988) was also shown

† To whom all correspondence should be sent.

0953-8984/92/286029+10$04.50

to melt from a superionic phase, and the less conclusive diffraction study of AgI by Howe (1988) have both supported this suggestion.

In this present neutron diffraction study, results for the three partial structure factors of CuBr have been obtained using the method of isotopic substitution of copper. The results are compared with those for CuCl in an attempt to understand the origins and controlling factors of the observed cation behaviour in molten salts that melt from a superionic phase. In particular, the effects of changing the anion species from chlorine to bromine can provide insight into the roles of ion size and ionicity.

2. Experimental details

Using the Faber–Ziman definition of total structure factors, a single neutron diffraction experiment on a liquid containing two atomic species, a and b, with concentrations C_a and C_b, yields

$$F(Q) = C_a^2 b_a^2 [S_{aa}(Q) - 1] + C_b^2 b_b^2 [S_{bb}(Q) - 1] + 2C_a C_b b_a b_b [S_{ab}(Q) - 1] \qquad (1)$$

where b_a and b_b are the coherent neutron scattering lengths of the two species and the $S_{\alpha\beta}(Q)$ are the partial structure factors. The total structure factor is the normalized differential scattering cross-section and is related to the experimentally determined sample cross-section by

$$F(Q) = \frac{1}{N}\frac{d\sigma}{d\Omega} - \sum C_\alpha \bar{b}_\alpha^2$$

where N is the number of atoms in the neutron beam. The pair distribution functions, $g_{\alpha\beta}(r)$, are related to the partial structure factors by Fourier sine transformation

$$g_{\alpha\beta}(r) = 1 + \frac{1}{2\pi^2 \rho r}\int Q[S_{\alpha\beta}(Q) - 1]\sin(Qr)\,dQ \qquad (2)$$

where ρ is the mean atomic number density. Fourier transformation of the total structure factors will produce total distribution functions, defined as

$$G(r) = 4\pi r\rho \sum C_\alpha C_\beta b_\alpha b_\beta [g_{\alpha\beta}(r) - 1] = \frac{2}{\pi}\int QF(Q)\sin(Qr)\,dQ. \qquad (3)$$

The total structure factors for four isotopically distinct samples of molten copper(I) bromide have been obtained by measuring their differential scattering cross-sections. The isotopic samples used were ^{63}CuBr, ^{65}CuBr, ^{mix}CuBr (defined in table 1) and natural CuBr. The different coherent scattering lengths for each copper isotope resulted in a set of equations for $F(Q)$ with different coefficients, from which the three partial structure factors were calculated. The copper isotopes that were used were chosen to give the optimum conditioning when determining the set of $S_{\alpha\beta}$ from the set of $F(Q)$s.

The isotopically enriched samples were prepared in powdered form by the isotopic preparation unit at Bristol University. They were then dried by heating carefully under vacuum to a temperature of 160 °C over a period of about seven days and at

Table 1. Parameters used for the data analysis of the four isotopic samples.

Isotope	Composition % ^{63}Cu	% ^{65}Cu	$\bar{b}_c$ (10^{-12} cm)†	σ_a (10^{-24} cm^2)† at 0.7 Å
Copper-63	99.72	0.28	0.644	1.75
Natural copper	69.17	30.83	0.772	1.47
Copper mix	54.2	45.8	0.834	1.34
Copper-65	0.39	99.61	1.059	0.85
Natural bromine			0.679	2.69

† From Sears (1984).

a pressure of 10^{-6}–10^{-5} Torr. The dried samples were then pre-melted and sealed into cylindrical fused silica containers of internal diameter 5 mm and wall thickness of 1 mm under half an atmosphere of argon.

The measurements were made using the D4B diffractometer at the Institut Laué–Langevin (ILL), Grenoble, (Institut Laué–Langevin 1988), using neutrons with a wavelength of 0.7 Å and a beam height of 35 mm. The samples were heated by a cylindrical vanadium foil furnace to a temperature of 515 °C, 23 °C above the melting point. In addition to the four samples, spectra were measured for an empty container and the empty furnace. Corrections were made for sample and container attenuation as well as multiple scattering.

Total structure factors were obtained from the measured scattering intensities for the four salts after subtraction of the corrected container and background scattering. Normalization was achieved by scaling the high-Q limit of the data to the self-scattering level, which is determined by the scattering cross-sections. The spectra measured by the two detector banks matched well over their region of overlap and were combined using a flux weighting method. This involved evaluating a weighted average with each data point being assigned a significance equal to $1/\sigma^2$, where σ is its error.

Table 1 lists the parameters used for the analysis and figure 1 shows the total structure factors obtained. In the absence of any density measurement for molten CuBr, the value chosen for the analysis was that used by Stafford *et al* (1990) for their simulation, $\rho_0 = 0.035$ atoms Å^{-3}. This was an estimate based on the densities of CuCl and AgI. The uncertainty introduced by this lack of knowledge of the density has been taken into account when determining structural parameters from these results. The total structure factors have been Fourier transformed to produce the total distribution functions of figure 2.

The four simultaneous equations for these samples, derived from equation (1) are

$$^{63}F(Q) = 0.104[S_{\mathrm{CuCu}}(Q) - 1] + 0.115[S_{\mathrm{BrBr}}(Q) - 1] + 0.219[S_{\mathrm{CuBr}}(Q) - 1] \tag{4}$$

$$^{\mathrm{nat}}F(Q) = 0.149[S_{\mathrm{CuCu}}(Q) - 1] + 0.115[S_{\mathrm{BrBr}}(Q) - 1] + 0.262[S_{\mathrm{CuBr}}(Q) - 1] \tag{5}$$

$$^{\mathrm{mix}}F(Q) = 0.174[S_{\mathrm{CuCu}}(Q) - 1] + 0.115[S_{\mathrm{BrBr}}(Q) - 1] + 0.283[S_{\mathrm{CuBr}}(Q) - 1] \tag{6}$$

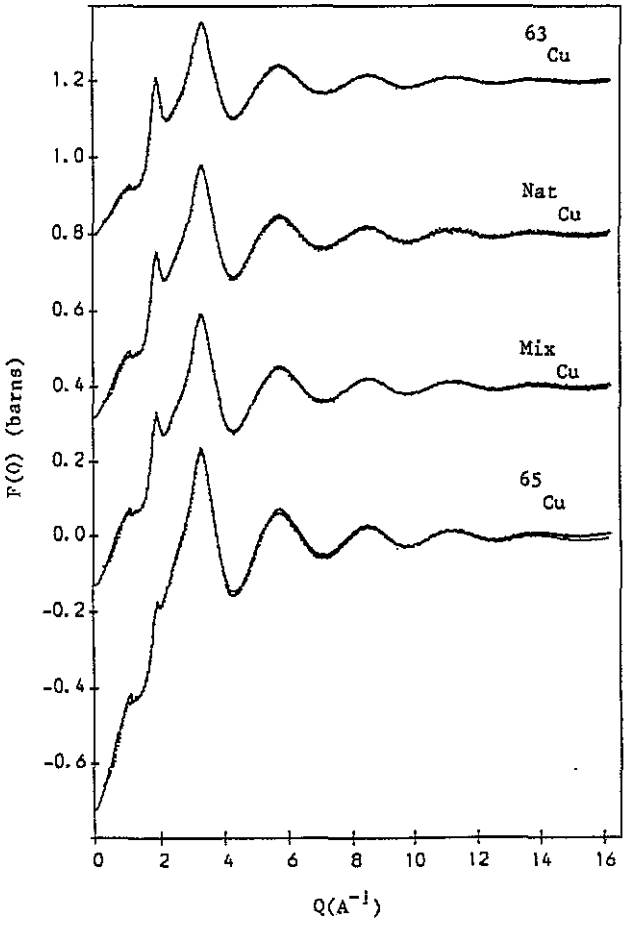

Figure 1. The normalized differential scattering cross-sections of the four CuBr samples (dots). The full lines are recombined from the partial structure factors. Each successive plot has been displaced by 0.4.

$$^{65}F(Q) = 0.280[S_{CuCu}(Q) - 1] + 0.115[S_{BrBr}(Q) - 1] + 0.360[S_{CuBr}(Q) - 1]. \tag{7}$$

For the separation of the partial structure factors from these total structure factors, equations (4), (6) and (7) give the best conditioning and were the ones that were used. The structure factor for the natural sample served as an independent check upon the accuracy of the partials obtained, which are shown in figure 3. When recombined with the coefficients of equations (4) to (7), these partials produced the full lines of figure 1, which compare well with the original total structure factors.

In order to Fourier transform these partial structure factors to obtain pair distribution functions, it was necessary to extrapolate the data at low Q to the long-wavelength limit at $Q = 0$. This was achieved with reference to the estimate of the isothermal compressibility of molten CuBr made by Takeda *et al* (1989) from their ultrasonic velocity measurements. Fortunately, because of the dependence on Q of equation (2), the distribution functions are insensitive to this region of Q-space. The values of $F(0)$ used were -0.40, -0.73, -0.54 and -0.49 for the ^{63}CuBr, ^{65}CuBr,

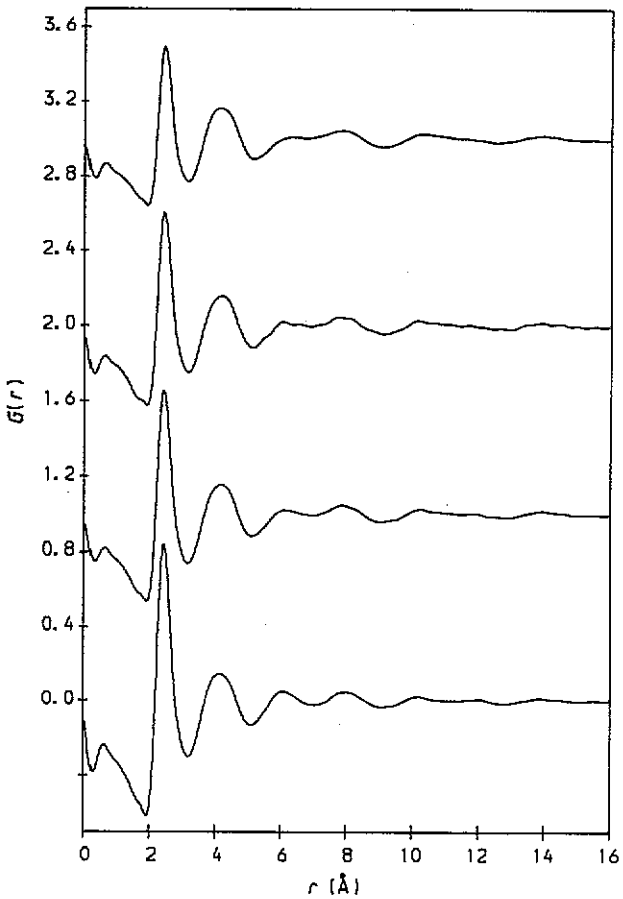

Figure 2. Total distribution functions for the four samples of molten CuBr. Each successive plot has been displaced by 0.5.

^{mix}CuBr and natural CuBr samples respectively.

The statistical accuracy of the three partial structure factors is inadequate for a direct Fourier transformation to real space. This is due to the relatively poor conditioning which results from the use of copper isotopes. It was, therefore, necessary to use a modification function of the form $\sin(\pi Q/Q_{max})/(\pi/Q_{max})$ prior to transformation, where Q_{max} is the upper limit for the integration in equation (2). This has the effect of reducing ripples in $g(r)$ which arise from the finite range and noise of the data. The distribution functions obtained by this method are shown as broken lines in figure 4. However, even with this use of a modification function, the effects of truncation and noise upon these transforms are severe. For this reason, the maximum-entropy method based upon the algorithm of Skilling and Bryan (1984) has also been used. The real-space, maximum-entropy solutions are obtained by iteration, from fitting their reverse Fourier transforms to the Q-space data, subject to a maximum-entropy constraint. These maximum-entropy solutions are shown as full lines in figure 4. The inverse transforms of these functions are the full lines of figure 3.

Table 2 summarizes the structural parameters that have been obtained from the

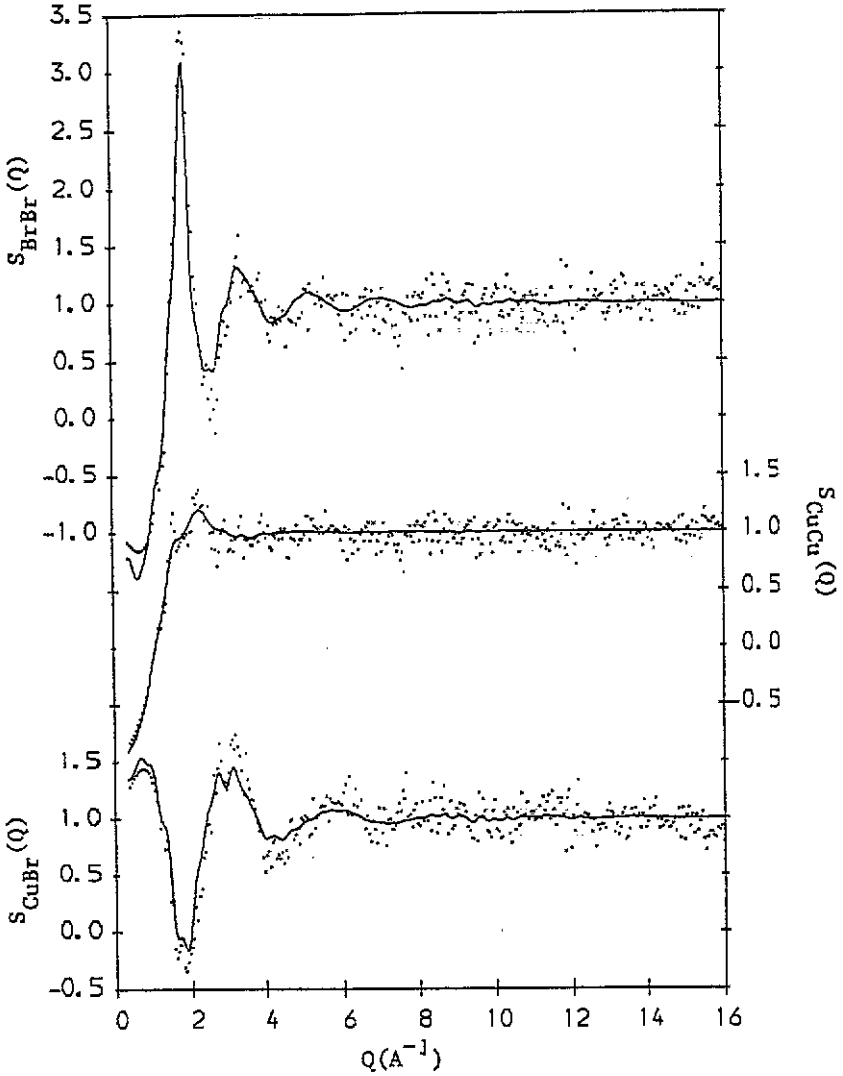

Figure 3. The three partial structure factors for molten CuBr (dots). The full lines are the back-transforms of the maximum-entropy solutions.

data and the Fourier transforms. The coordination numbers have been derived by integrating under the principal peaks in the $r^2 g_{\alpha\beta}(r)$ functions up to the first minimum.

3. Results

From an examination of the partial structure factors and distribution functions of figures 3 and 4 and the structural parameters of table 2, the following features are apparent.

(i) *The cation–anion structure.* The Cu–Br partial structure factor displays characteristics that are typical of an ionic liquid. In reciprocal space, the characteristic

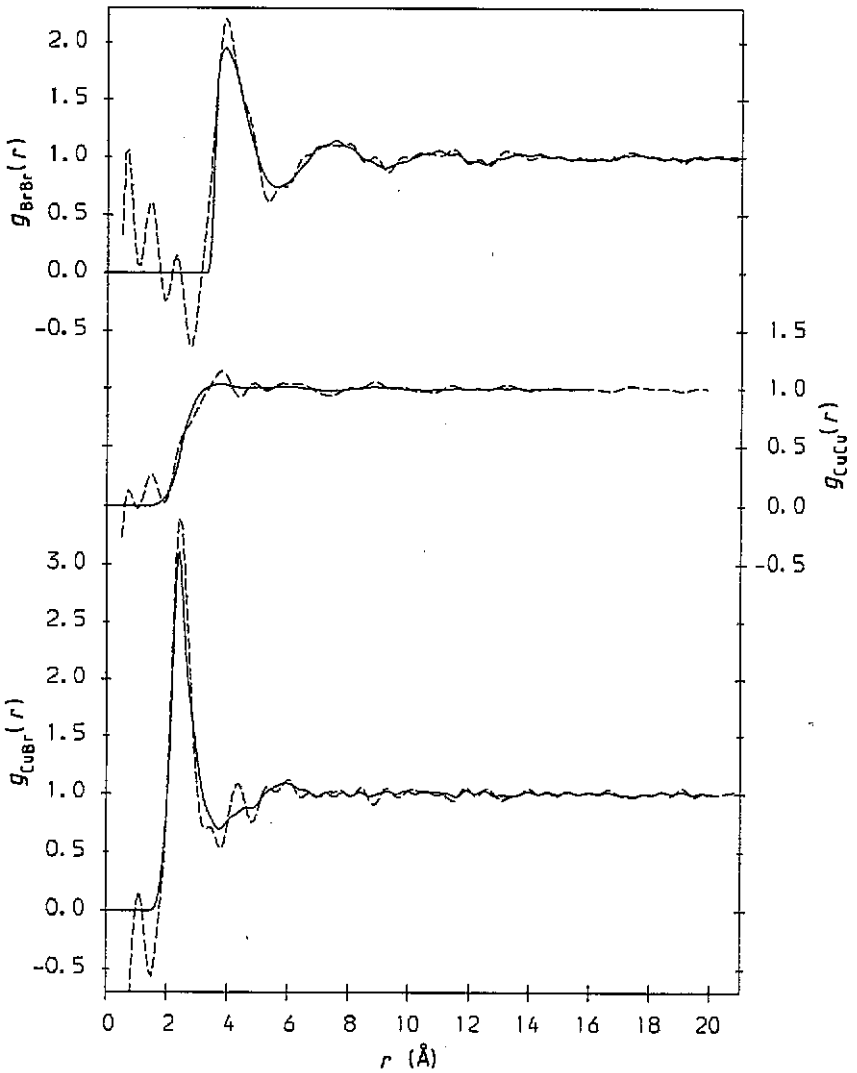

Figure 4. The three pair distribution functions for molten CuBr. The full lines are the maximum-entropy solutions and the broken lines are direct Fourier transforms of the partial structure factors.

'Coulomb dip' in $S_{CuBr}(Q)$ (indicative of charge ordering) is evident at $Q = 1.8$ Å^{-1}, and is approximately coincident with the principal peak in $S_{BrBr}(Q)$. In real space, the first peak in $g(r)$ is very well defined. It is narrow and is even higher than that published for CuCl, although both heights are likely to be limited by the real-space resolution.

(ii) *Tetrahedral coordination.* The coordination number of anions around cations is approximately 4, which compares with a value of 3 ± 0.7 for CuCl. In addition, the ratio of nearest-neighbour peak positions in $r^2 g_{BrBr}(r)$ and $r^2 g_{CuBr}(r)$ is 1.59 ± 0.03. This compares well with that expected for a perfect tetrahedron of 1.63, but is less than the value of 1.7 for CuCl, which was estimated from digitized plots of the data published by Eisenberg *et al.* It can be concluded therefore that

Table 2. Structural parameters for molten copper bromide.

	Cu–Br term	Br–Br term
Peak position in $g(r)$ (Å)	2.43 ± 0.02	3.89 ± 0.01
Peak height in $g(r)$	3.6 ± 0.7	2.4 ± 0.4
Trough position in $g(r)$ (Å)	3.78 ± 0.03	5.30 ± 0.02
Peak position in $r^2g(r)$ (Å)	2.50 ± 0.04	3.97 ± 0.03
Trough position in $r^2g(R)$ (Å)	3.21 ± 0.05	5.26 ± 0.02
Coordination number	3.63 ± 0.45	11.1 ± 0.07
$\bar{r}_{BrBr}/\bar{r}_{CuBr}$	1.59 ± 0.03	
Dip/peak position in $S(Q)$ (Å^{-1})	1.80 ± 0.04	1.88 ± 0.02

tetrahedral coordination of bromide ions around copper ions is the predominant local environment for molten CuBr, but not for CuCl.

(iii) *The anion–anion structure.* There is discernible structure in $g_{BrBr}(r)$ out to about 22 Å, which is further than that observed for $g_{CuBr}(r)$. Integration under the first peak of $r^2g_{BrBr}(r)$ yields a coordination number of about 12 nearest-neighbour anions. This compares with a coordination number of 8 for the high-temperature BCC α-phase of CuBr. These two facts imply a closely packed and 'stiff' anion structure in the liquid, similar to that found for CuCl. The observation of a significant change of the local structure upon melting is contrary to the suggestion of McGreevy and Pusztai (1990) that salts always melt to form local structures that are similar to those in the crystals from which they have melted.

(iv) *The cation–cation structure.* The Cu–Cu partial distribution function is even more featureless than that found in CuCl. This indicates a very high degree of mobility for the copper ions. Considerable first-shell penetration of copper ions is evident. On average, $25 \pm 5\%$ of all ions within the first shell around a cation (defined by the first minimum in $r^2g_{CuBr}(r)$) are copper rather than bromine ions.

Clearly molten CuCl is not unique in possessing a 'gas-like' distribution of mobile cations within a well defined structure of anions; CuBr has a very similar structure.

4. Discussion

An attempt to model the anomalous structure of molten CuCl has been carried out by Ginoza *et al* (1987) using ionic potentials and the mean spherical approximation. They had great difficulty in reproducing even the broad features of the experimental data. In particular, they could only obtain a $g_{++}(r)$ that was much less structured than $g_{--}(r)$ by using a very low value of $0.16e$ for the ionic charge and a cation-to-anion size ratio of 0.36 instead of the Pauling value of 0.53. This combination appears at odds with the naive expectation that reduced charge transfer would be associated with an increase in cation-to-anion size ratio. Furthermore, the modelled $g_{++}(r)$ still possessed considerably more amplitude of oscillation than the experimentally determined function. Similarly, Stafford *et al* (1990) used ionic potentials in both HNC and molecular dynamics methods in an attempt to simulate the structures of the copper halides and AgI, all of which exhibit superionic behaviour in their high-temperature solid phases. Once again they adopted a reduced effective charge, this time of $0.5e$, but their ion sizes were obtained from crystal lattice constants. In their comparison with the experimentally determined partial radial distribution functions

for CuCl, none of the three partials was an acceptable fit. However, $g_{CuCu}(r)$ was substantially less structured than $g_{ClCl}(r)$, in accord with experiment, but was still too structured when compared with the experimental function.

Clearly, both reducing the ion size ratio from its Pauling value, to perhaps unrealistically low values, and reducing the effective ionic charge have produced some success in modelling the structure of molten copper chloride. However, no simulation involving either or both of these features has yet been successful for CuCl.

Comparison of our results for molten CuBr at 515 °C with the published results obtained by Eisenberg *et al* (1982) for CuCl, at a temperature that is only 15 °C lower, reveals a cation structure that is even less ordered for CuBr than for CuCl with similar first-shell penetration. This is consistent with there being a smaller charge transfer between ions in CuBr than there is in CuCl and with the changes in electronegativity. It seems sensible, therefore, to look for distinctive features in the local short-range structure of the two salts which might arise from the reduced charge transfer.

The nearest-neighbour distances between the halide ions and between the copper and halide ions (defined by the principal peak positions in $r^2g(r)$) are listed in table 3 for molten CuCl and CuBr, together with the Pauling ionic radii. In both cases, the Cu–X distance (X=Cl, Br) is approximately 0.87 times the sum of the two ionic radii. This similarity is expected, since the short-range repulsion must be the most significant force in determining the Cu–X interionic distance between ions that are in contact. However, the X–X nearest-neighbour distance does not scale with either the sum of the two ionic radii or the anion diameters. Comparison of the peak positions with the sum of the ionic radii suggests that in CuBr, the Br ions are more 'in contact' with one another than the Cl ions are in CuCl. This observation is consistent with a reduction in the Coulombic force of repulsion for CuBr when compared with CuCl and therefore with reduced charge transfer. A similar trend for the anion–anion distances compared with the anion diameters was observed for the nickel halide series (Wood and Howe 1988) where similar models of charge transfer were discussed.

Table 3. Comparison of nearest-neighbour distances compared with Pauling ion radii for CuCl and CuBr.

	CuCl		CuBr	
	Cu–Cl	Cl–Cl	Cu–Br	Br–Br
$\bar{r}_{\alpha\beta}/(\sigma_+ + \sigma_-)$	0.88 ± 0.01	1.47 ± 0.03	0.86 ± 0.02	1.36 ± 0.02
$\bar{r}_{\alpha\beta}/2\sigma_-$	0.67 ± 0.01	1.12 ± 0.03	0.64 ± 0.01	1.02 ± 0.02

It is useful to consider the effect of reduced charge transfer upon the mobility of the cations. The reduction in magnitude of the charge-dependent forces (Coulomb, Van der Waals and any polarization forces) should lead to a reduction in the depth of the potential wells between which the mobile cations hop, and therefore to an increase in cation mobility. The Monte Carlo simulation by Margheritis (1989) of the superionic conductor AgI in its molten phase, which used the potential form suggested by Parrinello *et al* (1983), showed a loss of structural ordering of the cation species and of the cation–anion correlation upon reduction of the magnitude of the ionic charge. This result is supported by the other simulation results and suggests enhanced mobility of the cations upon reduction of ionic charge.

5. Summary

In conclusion, the results presented in this paper support the suggestion made by Stafford *et al* (1990) that all of the copper halides should have similar structural characteristics to CuCl. Both CuCl and CuBr exhibit a considerable asymmetry between Cu–Cu and X–X pair distribution functions and a large degree of first-shell penetration by copper ions. In contrast to CuCl however, CuBr has tetrahedral rather than threefold coordination of cations by anions and melts to form an anion structure that is markedly different from the one that it has in its solid-state high-temperature phase. The loss of structural ordering in $g_{CuCu}(r)$ indicates a high cation mobility in both salts, with the mobility in CuBr exceeding that in CuCl. There is a large degree of first-shell penetration by cations in both salts. The penetration in CuBr is similar to that in CuCl in spite of an increase in the coordination number of anions.

These facts are consistent with a significantly reduced charge transfer in both of these systems with the transfer in CuBr being even less than that in CuCl.

Acknowledgments

We wish to thank Mr Y Badyal and the staff at the ILL (Grenoble), in particular Dr P Chieux, for their help in conducting this experiment. We are also grateful to Mr P Gullidge, formerly of the University of Bristol, for his assistance in the preparation of the isotopic samples. We acknowledge the support given to this work by the Science and Engineering Research Council.

References

Boyce J B and Mikkelsen J C 1977 *J. Phys. C: Solid State Phys.* **10** L41
Edwards F G, Enderby J E, Howe R A and Page D I 1975 *J. Phys. C: Solid State Phys.* **8** 3483
Eisenberg S, Jal J-F, Dupuy J, Chieux P and Knoll W 1982 *Phil. Mag.* A **46** 195
Ginoza M, Nixon J H and Silbert M 1987 *J. Phys. C: Solid State Phys.* **20** 1005
Howe M A 1988 *PhD Thesis* Oxford University
Institut Laué–Langevin 1988 *Guide to Neutron Research Facilities at the ILL, Grenoble*
Margheritis C 1989 *Z. Naturf.* a **44** 567
McGreevy R L and Pusztai L 1990 *Proc. R. Soc.* **430** 241
Page D I and Mika K 1971 *J. Phys. C: Solid State Phys.* **4** 3034
Parrinello M, Rahman A and Vashishta P 1983 *Phys. Rev. Lett.* **50** 1073
Powles J G 1975 *J. Phys. C: Solid State Phys.* **8** 895
Sears V F 1984 *Atomic Energy of Canada Ltd Report* AECL-8490
Skilling J and Bryan R K 1984 *Mon. Not. R. Astron. Soc.* **211** 111
Stafford A J, Silbert M, Trullàs J and Giró A 1990 *J. Phys.: Condens. Matter* **2** 6631
Takeda S, Shirakawa Y, Takesawa K, Harada S and Tamaki S 1989 *J. Phys. Soc. Japan* **58** 4007
Wood N D 1988 private communication
Wood N D and Howe R A 1988 *J. Phys. C: Solid State Phys.* **21** 3177
Wood N D, Howe R A, Newport R J and Faber J Jr 1988 *J. Phys. C: Solid State Phys.* **21** 669